CHEMISTRY OF MATERIALS
Article

Chem. Mater. **2010,** *22,* 1429–1436 1429
DOI:10.1021/cm902834a

Multifunctional Electrospun Fabrics via Layer-by-Layer Electrostatic Assembly for Chemical and Biological Protection

Liang Chen,[†] Lev Bromberg,[†] Jung Ah Lee,[†] Huan Zhang,[†] Heidi Schreuder-Gibson,[‡] Phillip Gibson,[‡] John Walker,[‡] Paula T. Hammond,[†] T. Alan Hatton,*[,†] and Gregory C. Rutledge*[,†]

[†]*Department of Chemical Engineering, Massachusetts Institute of Technology, 77 Massachusetts Avenue, Cambridge, Massachusetts 02139, and* [‡]*US Army Research, Development and Engineering Command, Natick Soldier Research, Development & Engineering Center, Natick, Massachusetts 01760*

Received September 10, 2009. Revised Manuscript Received November 27, 2009

Breathable chemical and biological detoxifying protective fabrics are obtained via functionalization of electrospun fiber mats using a layer-by-layer electrostatic assembly technique. The chemically reactive polyanion, poly(*N*-hydroxyacrylamide) or poly(hydroxamic acid) (PHA), and bactericidal polycation, poly(*N*-vinylguanidine) (PVG), were synthesized and assembled electrostatically to generate multifunctional coatings on prefabricated polyacrylonitrile (PAN) fiber mats. Reactivity of PHA in the hydrolysis of diisopropyl fluorophosphate (DFP), a close analog of the chemical warfare agent sarin, was demonstrated. The DFP degradation rate with PHA is comparable to that with compounds such as isonicotinhydroxamic acid methiodide, an efficient catalyst of organophosphate ester hydrolysis. Protective fabrics functionalized with PVG/PHA layers are able to degrade DFP mists, with DFP hydrolysis rates 60-fold higher than those with unmodified fabrics under identical conditions. Fabrics modified with PVG/PHA layers are bactericidal against *E. coli* and *S. epidermidis*. Breathability of functionalized fiber mats as protective fabrics was evaluated versus standard reference fabrics.

1. Introduction

The increased concern over exposure to the hazards of pesticides, nerve agents, and chemical and biological toxins, along with the growing chemical and biological threats due to intentional or accidental release of toxic agents, motivates the development of countermeasures to provide effective protection for military personnel and emergency responders. Currently, the protective clothing systems such as hazardous material (HAZMAT) suits or joint service lightweight integrated suit technology (JSLIST) are widely used to achieve full protection. These protective systems are based upon either full barrier protection through blocking contaminant permeation or on air-permeable adsorptive protective overgarments in which all the toxins are adsorbed on contact.[1] High thermal loads from poor water vapor permeability and excess insulation as well as weight and bulkiness of these protective fabrics and suits impair a wearer's performance. Recently, protective fabrics have been based on selectively permeable membranes, which allow for permeation of water vapor while remaining resistant to the permeation of organic molecules.[2] The new generation of protective fabrics is envisioned not only to absorb or block toxic chemical and biological agents but also to detoxify them to reduce the risk of secondary contamination.[1]

Electrospinning is a fiber-forming process that employs electrostatic forces to stretch a jet of polymer solution or melt, to produce continuous fibers with diameters ranging from micrometers down to several nanometers.[3−10] The ease of implementation as well as the remarkable properties of electrospun fiber mats, such as small fiber size, high specific surface area, high porosity, and low fabric weight, have inspired the use of the electrospun fiber mats in a broad range of applications, including scaffolds in tissue engineering, composite materials, filters, sensors, and energy storage devices.[11−17] The potential for application

*Corresponding authors. E-mail addresses: tahatton@mit.edu (T.A.H.) and rutledge@mit.edu (G.C.R.).

(1) Schreuder-Gibson, H. L.; Truong, Q.; Walker, J. E.; Owens, J. R.; Wander, J. D.; Jones, W. E. *MRS Bull.* **2003**, *28*, 574.
(2) Wilusz, E.; Truong, Q. T.; Rivin, D.; Kendrick, C. E. *Polym. Mat. Sci. Eng.* **1997**, *77*, 365.
(3) Dzenis, Y. *Science* **2004**, *304*, 1917.
(4) Rutledge, G. C.; Fridrikh, S. V. *Adv. Drug Delivery Rev.* **2007**, *59*, 1384.
(5) Reneker, D. H.; Yarin, A. L. *Polymer* **2008**, *49*, 2387.
(6) Reneker, D. H.; Chun, I. *Nanotechnology* **1996**, *7*, 216.
(7) Greiner, A.; Wendorff, J. H. *Angew. Chem., Int. Ed.* **2007**, *46*, 5670.
(8) Li, D.; Xia, Y. *Adv. Mater.* **2004**, *16*, 1151.
(9) Ramakrishna, S.; Fujihara, K.; Teo, W. E.; Yong, Y.; Ma, Z. W.; Ramaseshan, R. *Mater. Today* **2006**, *9*, 40.
(10) Ramakrishna, S.; Fujihara, K.; Teo, W.-E.; Lim, T.-C.; Ma. Z. *An Introduction to Electrospinning and Nanofibers*; World Scientific Publishing Company: Singapore, 2005.
(11) Ma, Z. W.; Kotaki, M.; Inai, R.; Ramakrishna, S. *Tissue Eng.* **2005**, *11*, 101.
(12) Roso, M.; Sundarrajan, S.; Pliszka, D.; Ramakrishna, S.; Modesti, M. *Nanotechnology* **2008**, *19*, 285707.
(13) Yoon, K.; Hsiao, B. S.; Chu, B. *J. Mater. Chem.* **2008**, *18*, 5326.
(14) Thavasi, V.; Singh, G.; Ramakrishna, S. *Energy Environ. Sci.* **2008**, *1*, 205.
(15) Kim, I. D.; Rothschild, A.; Lee, B. H.; Kim, D. Y.; Jo, S. M.; Tuller, H. L. *Nano Lett.* **2006**, *6*, 2009.

Published on Web 01/07/2010

of electrospun fiber mats in protective clothing was demonstrated by Gibson and co-workers.[18−20] They showed that lightweight electrospun fabrics exhibit higher breathability than do barrier materials while displaying better airflow resistance and enhanced aerosol particle retention compared to current commercially available membranes. "Breathability" in this instance is defined as transmission of water vapor but not liquid water. In addition, Obendorf et al. showed that laminated fabrics with electrospun polypropylene fiber layers significantly limit the penetration of liquid pesticides while still maintaining good water vapor permeability.[21] The combination of high breathability and efficient barrier properties of electrospun fabrics makes them promising candidates for the next generation of protective clothing. Moreover, the high specific surface areas of electrospun fiber mats allow attachment of functional compounds to obtain chemical or biological detoxifying protective clothing. Ramakrishna et al. successfully electrospun fibers with a reactive compound, (3-carboxy-4-iodosobenzyl) oxy-β-cyclodextrin, and showed that these reactive fabrics can decompose paraoxon, an organophosphate pesticide.[22] In another study, electrospun zinc titanate nanofibers were tested as reactive sorbents capable of detoxifying nerve and mustard agent simulants.[23] Various biocides such as silver nanoparticles, quaternary ammonium salts or their derivatives, compounds with biguanide groups, and *N*-halamine have been incorporated into electrospun fiber membranes to serve as antimicrobial filters or to create biological protective clothing.[24−28]

We have studied chemical methods to counteract nerve agents and remediate organophosphate (OP) contamination by means of nanoparticles, polymers and nanofibers functionalized by α-nucleophilic agents.[29−33] Fiber mats functionalized with α-nucleophilic oxime moieties were prepared by either electrospinning blends of polyacrylamidoxime (PAAO) and polyacrylonitrile (PAN) or surface oximation of prefabricated PAN fiber mats and demonstrated to possess a pronounced capability to hydrolyze chemical nerve agent simulants in the presence of moisture.[32,33] The fiber postspin modification strategy has the advantages of higher surface density of oxime functional groups, enhanced reactivity, and ease of implementation compared to the PAN/PAAO blending strategy.[32] The layer-by-layer (LbL) electrostatic assembly technique offers another strategy for electrospun fiber surface functionalization. The LbL electrostatic assembly is a simple, versatile, and inexpensive approach to generate functional multilayer thin film coatings on surfaces.[34,35] The utilization of electrospun fiber mats as substrates for LbL-based functional coatings enhances the functioning of multilayered coatings by significantly increasing the specific surface area of substrates.[36−39] Wang et al. showed that a fluorescent probe assembled by the LbL method onto electrospun cellulose acetate membranes resulted in a dramatic increase in sensitivity of optical sensors.[36] For the application in protective fabrics, Lee et al. demonstrated that electrospun fibers used as the substrate for titanium dioxide nanoparticle coatings resulted in increased specific substrate surface areas of about 10^4 that of the flat film, which enhanced photocatalytic decomposition of toxic industrial chemicals.[38] In addition, Krogman et al. employed a newly developed spray-assisted LbL assembly technique to functionalize electrospun nylon fibers with titanium dioxide nanoparticles for protective fabrics, in which they could obtain conformal coatings or bridge the surface voids by controlling the spraying conditions; they demonstrated that they could achieve LbL-functionalized fiber mats with improved photocatalytic capability without sacrificing water vapor permeability or breathability of the electrospun fiber mats.[39] Another advantage of the LbL electrostatic assembly is that, by selecting appropriate polyelectrolytes of opposite charges and varying functionalities, one can generate multifunctional electrospun, fiber-based protection fabrics for both chemical and biological protection. In this study, a nucleophilic and chemically reactive polyanion, polyhydroxamic acid (PHA), and an antimicrobial polycation, poly(*N*-vinylguanidine) (PVG), were synthesized and assembled onto prefabricated PAN fiber mats. The performance of the functionalized mats in OP decomposition was tested with diisopropyl fluorophosphate (DFP), a widely used simulant for G-type nerve agents.[40] The antibacterial properties of these functionalized mats were examined with

(16) Thandavamoorthy, S.; Bhat, G. S.; Tock, R. W.; Parameswaran, S.; Ramkumar, S. S. *J. Appl. Polym. Sci.* **2005**, *96*, 557.
(17) Thandavamoorthy, S.; Gopinath, N.; Ramkumar, S. S. *J. Appl. Polym. Sci.* **2006**, *101*, 3121.
(18) Gibson, P.; Schreuder-Gibson, H. L.; Rivin, D. *Colloids Surf. A* **2001**, *187*, 469.
(19) Gibson, P. W.; Schreuder-Gibson, H. L.; Rivin, D. *AIChE J.* **1999**, *45*, 190.
(20) Gibson, H. L.; Gibson, P.; Senecal, K.; Sennett, M.; Walker, J.; Yeomans, W.; Ziegler, D.; Tsai, P. P. *J. Adv. Mater.* **2002**, *34*, 44.
(21) Lee, S.; Obendorf, S. K. *J. Appl. Polym. Sci.* **2006**, *102*, 3430.
(22) Ramaseshan, R.; Sundarrajan, S.; Liu, Y.; Barhate, R. S.; Lala, N. L.; Ramakrishna, S. *Nanotechnology* **2006**, *17*, 2947.
(23) Ramaseshan, R.; Ramakrishna, S. *J. Am. Ceram. Soc.* **2007**, *90*, 1836.
(24) Lala, N. L.; Ramaseshan, R.; Bojun, L.; Sundarrajan, S.; Barhate, R. S.; Ying-jun, L.; Ramakrishna, S. *Biotechnol. Bioeng.* **2007**, *97*, 1357.
(25) Fu, G.-D.; Yao, F.; Li, Z.; Li, X. *J. Mater. Chem.* **2008**, *18*, 859.
(26) Fan, L.; Du, Y.; Zhang, B.; Yang, J.; Zhou, J.; Kennedy, J. F. *Carbohydr. Polym.* **2006**, *65*, 447.
(27) Chen, L.; Bromberg, L.; Hatton, T. A.; Rutledge, G. C. *Polymer* **2008**, *49*, 1266.
(28) Tan, K.; Obendorf, S. K. *J. Membr. Sci.* **2007**, *305*, 287.
(29) Bromberg, L.; Schreuder-Gibson, H.; Creasy, W. R.; McGarvey, D. J.; Fry, R. A.; Hatton, T. A. *Ind. Eng. Chem. Res.* **2009**, *48*, 1650.
(30) Bromberg, L.; Zhang, H.; Hatton, T. A. *Chem. Mater.* **2008**, *20*, 2001.
(31) Bromberg, L.; Hatton, T. A. *Ind. Eng. Chem. Res.* **2005**, *44*, 7991.
(32) Chen, L.; Bromberg, L.; Schreuder-Gibson, H.; Walker, J.; Hatton, T. A; Rutledge, G. C. *J. Mater. Chem.* **2009**, *19*, 2432.
(33) Chen, L.; Bromberg, L.; Hatton, T. A.; Rutledge, G. C. *Polymer* **2007**, *48*, 4675.
(34) Hammond, P. T. *Adv. Mater.* **2004**, *16*, 1271.
(35) Decher, G. *Science* **1997**, *277*, 1232.
(36) Wang, X.; Kim, Y.-G.; Drew, C.; Ku, B.-C.; Kumar, J.; Samuelson, L. A. *Nano Lett.* **2004**, *4*, 331.
(37) Yang, G.; Gong, J.; Yang, R.; Guo, H.; Wang, Y.; Liu, B.; Dong, S. *Electrochem. Commun.* **2006**, *8*, 790.
(38) Lee, J. A.; Krogman, K. C.; Ma, M.; Hill, R. M.; Hammond, P. T.; Rutledge, G. C. *Adv. Mater.* **2009**, *21*, 1252.
(39) Krogman, K. C.; Lowery, J. L.; Zacharia, N. S.; Rutledge, G. C.; Hammond, P. T. *Nat. Mater.* **2009**, *8*, 512.
(40) Yang, Y.-C.; Baker, J. A.; Ward, J. R. *Chem. Rev.* **1992**, *92*, 1729.

Scheme 1. Synthesis of Polyhydroxamic Acid

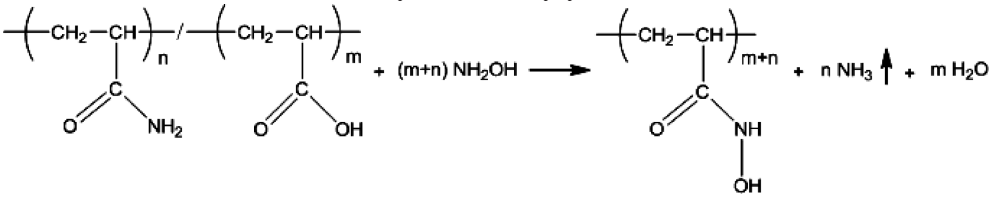

Escherichia coli (*E. coli*) and *Staphylococcus epidermidis* (*S. epidermidis*), gram-negative and gram-positive microorganisms, respectively.

2. Experimental Method

Materials. Polyacrylonitrile (PAN) (M_w 150 kDa) was purchased from Scientific Polymer Products Inc. (Ontario, NY) and used as received. Poly(acrylamide-*co*-acrylic acid) (M_w 200 kDa, acrylamide 20 wt %), diisopropyl fluorophosphate (99%, DFP), hydroxylamine hydrochloride (99%), cyanamide (50 wt % in water), and *N*,*N*-dimethylformamide (DMF) were all obtained from Sigma-Aldrich Chemical Co. (St. Louis, MO) and used as received. Lupamin 9095 (20−22% aqueous solution of polyvinylamine, average molecular weight 340 kDa) was kindly supplied by BTC (a specialty chemical distribution group of BASF, Germany). The porous expanded polytetrafluoroethylene (ePTFE) membrane was obtained from GE Energy (Lee's Summit, MO). The ePTFE membrane is supplied with a conformal oleophobic coating applied with a supercritical carbon dioxide process. The ePTFE membrane is approximately 0.02 mm thick, with an areal density of 0.0023 g/m^2 and porosity of about 50%. Bacteria *E. coli* (ATCC no. 67876) and *S. epidermidis* (ATCC no. 35984) were purchased from ATCC (Manassas, VA) and stored at −80 °C prior to use.

Electrospinning. PAN solutions in DMF (10 wt %) were prepared by dissolving the polymer at 50−70 °C followed by stirring at room temperature. The PAN solutions were electrospun into fiber mats using a home-built parallel plate apparatus.[41] The applied voltage (28−30 kV), the flow rate (0.015 mL/min), and the distance between the upper electrode and grounded collector (∼30 cm) were adjusted to stabilize the polymer jet to obtain fiber mats on the grounded collector.

Polymer Synthesis. *Synthesis of Poly*(*N-hydroxyacrylamide*) *or Polyhydroxamic Acid* (*PHA*). Scheme 1 shows oximation of poly(acrylamide-*co*-acrylic acid) to poly(*N*-hydroxyacrylamide (PHA) by hydroxylamine. Poly(acrylamide-*co*-acrylic acid) was mixed with excess hydroxylamine hydrochloride in deionized water. The resulting solution was stirred for 1 day at 70 °C and then an aqueous solution of sodium hydroxide was added followed by stirring for 3 days at room temperature to convert the polymer completely into PHA. Conversion of poly(acrylic acid) and polyacrylamide into PHA by hydroxylamine is well-documented.[29,42,43] Release of ammonia by bubbling was observed. The solution was then frozen at −80 °C and lyophilized. The resultant PHA was dissolved in deionized water, dialyzed against excess deionized water, and lyophilized. Fourier transform infrared (FTIR) (KBr, cm^{-1}): 3600 (broad, −NHOH), 3430 (broad, OH stretching), 3210 (amide NH stretching), 1630 (CO−NH bending), 1450 (CH_2 scissor bending), 1425 (C−N stretching).

Scheme 2. Synthesis of Poly(*N*-vinylguanidine)

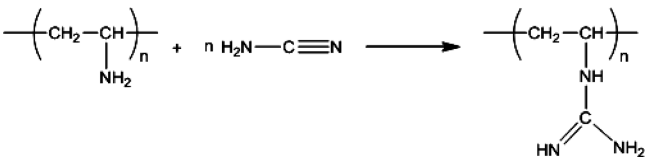

Synthesis of Poly(*N-vinylguanidine*) (*PVG*). Polyvinylamine (90% hydrolyzed) received as Lupamin 9095 was 100% hydrolyzed by 37% hydrochloric acid at 80 °C followed by polymer purification by precipitation into 2 M NaOH and dialysis (molecular weight cutoff, 12−14 kDa) and drying. Then, polyvinylamine was completely guanidinylated by cyanamide following the previously described procedure.[44] Scheme 2 shows the conversion of polyvinylamine to poly(*N*-vinylguanidine) by guanidinylation. FTIR (KBr): 957 cm^{-1} (C—N stretching), 1510 cm^{-1} (C—N stretching), 1610 cm^{-1} (NH, NH_2 deformation), 1670 cm^{-1} (C=N stretching), 2940 cm^{-1} (aliphatic CH_2 stretching). ^{13}C NMR (D_2O, ppm): 151.6 (C in the guanidinium group), 45.0 (methylene C in backbone), 35.5 (methane C in backbone).

LbL Assembly Coating. Aqueous solutions of PHA and PVG (10 mM, pH 9) were prepared and used for LbL assembly. Electrospun PAN fiber mats were plasma treated for 1 min (Harrick PDC-32G, Harrick Plasma Inc.) prior to LbL deposition. A Carl Zeiss DS50 programmable slide stainer was used for LbL deposition. Multilayer polyelectrolyte coatings on PAN fibers were produced by alternately dipping the fiber mat in 10 mM PVG and PHA aqueous solutions at room temperature. The dipping time in each polyelectrolyte solution was 60 min, followed by rinse in deionized water for 3 min.

Characterization. The fiber morphology was visualized by scanning electron microscopy (SEM, JEOL-6060). FTIR spectra were measured using a Nicolet 8700 spectrometer (Thermo Scientific Corp.) in the absorbance mode by accumulation of 256 scans with a resolution of 4 cm^{-1}. A Krato Axis Ultra Imaging XPS spectrometer (Kratos Analytical Co.) equipped with a monochromatized Al Kα X-ray source was used to analyze the surface chemistry of LbL-coated fibers. The takeoff angle relative to the sample substrate was set at 20°. ^{13}C NMR spectra were carried out using a Bruker Avance 400 spectrometer operating at 100.61 MHz for ^{13}C at room temperature. Proton decoupling was applied, and 15 000−20 000 scans were collected.

Permeability Testing. Water vapor diffusion and gas convection properties of functionalized electrospun PAN fiber mats were measured at 30 °C using an automated dynamic moisture permeation cell (DMPC) system.[45−47] The test fiber sample was

(41) Shin, Y. M.; Hohman, M. M.; Brenner, M. P.; Rutledge, G. C. *Polymer* **2001**, *42*, 9955.
(42) Zhang, J.-F.; Hu, Y.-H.; Wang, D.-Z. *J. Cent. South Univ. Technol.* **2002**, *9*, 177.
(43) Domb, A. J.; Cravalho, E. G.; Langer, R. J. *Polym. Sci., Pt A: Polym. Chem.* **1988**, *26*, 2623.
(44) Bromberg, L.; Hatton, T. A. *Polymer* **2007**, *48*, 7490.
(45) Gibson, P. W. *J. Coated Fabrics* **1999**, *28*, 300.
(46) Gibson, P. *J. Polym. Test.* **2000**, *19*, 673.
(47) Gibson, P. W.; Rivin, D.; Kendrick, C. *Int. J. Clothing Sci. Technol.* **2000**, *12*, 96.

placed between two chambers. The sample area (A) was about 10 cm^2. Air at two different relative humidities flows over the two sides of the test sample. For the water vapor diffusion test, the pressure difference across the membrane was maintained at zero; transport of water vapor proceeds by pure diffusion under these conditions. Relative humidities on both sides of the sample were increased at each set point to maintain a constant relative humidity difference of 0.5, while increasing the mean relative humidity (average of the relative humidity on the two sides of the sample) from 0.3 to 0.7. By measuring water vapor concentrations (C_{in} and C_{out}) and flowrates of the gas streams, one can determine the flux and the diffusion resistivity of water vapor transported through the test sample based on the following equation:[18]

$$N = \frac{Q(C_{out} - C_{in})}{A} = \frac{\Delta \bar{C}}{LR_{water}}$$

where N is the flux of the water vapor transported through the test sample; Q is the flow rate of the top or bottom gas stream; C_{in} and C_{out} are the measured inlet and outlet water vapor concentrations in either the top or the bottom gas stream; A is the area of the test sample; $\Delta \bar{C}$ is the log mean water vapor concentration difference between top and bottom gas streams at the inlet and exit of the cell; L is the thickness of the test sample; R_{water} is the water vapor diffusion resistivity. The thickness of untreated PAN fiber mats and the functionalized PAN fiber mats is 120 ± 40 and 90 ± 20 μm, respectively.

For the airflow resistance test, the air pressure difference was varied systematically across the test sample to produce convective flow through the test membrane; then one can accordingly obtain the airflow rate through the test sample by measuring the difference between inlet and outlet airflow rate in either the top or the bottom chamber. According to Darcy's law for a porous membrane, the airflow resistivity can be determined by the following equation:[18]

$$R_{air} = \frac{A\Delta p}{\mu QL}$$

where A is the area of the test sample; Δp is the pressure drop through the test sample; μ is the gas dynamic viscosity; Q is the airflow rate through the membrane; L is the thickness of the test sample; R_{air}, the apparent airflow resistivity, is the inverse of airflow permeability.

Kinetics of DFP Degradation. The kinetics of DFP degradation hydrolyzed by PHA in aqueous solutions was assessed by liquid state ^{31}P NMR spectrometry using a Varian 500 spectrometer operating at 202.46 MHz. The reaction milieu consisted of 50 mM of TES buffer to keep the solution pH constant at 7 and 20% (by volume) of deuterium oxide for signal locking. The spectra were recorded at ambient temperature (25 °C) by accumulation of 64 scans. The reaction time was taken to be the midpoint of the acquisition period.

Degradation of DFP mists on PVG/PHA-functionalized fiber mats was monitored by solid-state high-resolution magic angle spinning (HRMAS) ^{31}P NMR using a Bruker Avance 400 spectrometer (161.98 MHz for ^{31}P) as described previously.[32] The water content of the fiber mats, C_w, defined as the weight ratio of absorbed water to dry fiber mat, was maintained at 1.30 wt/wt in this work. The spectra were recorded at ambient temperature (21 °C) by accumulation of 64 scans. Triphenyl phosphate (TPP) in deuterated chloroform was used as an external reference for both liquid and solid state ^{31}P NMR measurements.

Antibacterial Tests. The antibacterial properties of the functionalized fiber mats were tested using the procedure of Tiller and co-workers,[48] with modifications. Briefly, *E. coli* and *S. epidermidis* were cultured overnight in Luria−Bertani (LB) broth and diluted in phosphate buffer solution (PBS, pH 7) to approximately 10^4−10^5 cells/mL. The bacterial suspension was then sprayed onto a functionalized fiber mat (6 cm × 4 cm) and a control fiber mat (6 cm × 4 cm) in a fume hood using a commercial chromatography sprayer. After drying for several minutes, the fiber mats were placed on top of the growth agar plates. The plates were inverted and incubated at 37 °C for 16−20 h. The number of viable colonies was counted visually, and the reduction in the number of viable bacteria colonies was averaged over three experiments.

3. Results and Discussion

DFP Degradation Mediated by PHA. Hydroxamic acid is a reactive α-nucleophile, capable of hydrolysis of organophosphate (OP) esters.[29,49,50] Hydrolytic destruction of OPs by low molecular weight hydroxamates has been established.[51,52] However, until recently,[29] little work has been done to study the action of polymers with hydroxamic acid groups, such as polyhydroxamic acid (PHA), in the degradation of OPs. In this work, the capability of PHA to decompose DFP, a common simulant for G-type nerve agents, in aqueous solution was evaluated.

Hydrolytic decomposition of DFP in aqueous solution in the presence of PHA was monitored by ^{31}P NMR spectroscopy. All the experiments were conducted under conditions of excess hydroxamic acid relative to the substrate ($[HA]_o > [DFP]_o$) with pH maintained constant at 7.0 using 50 mM TES buffer. Figure 1 shows a typical series of NMR spectra of DFP degradation mediated by PHA in aqueous solution as a function of time. Doublet signals at 4.6 and 9.4 ppm are attributed to the reactant, DFP, due to the splitting of the ^{31}P signal from the coupling of the P−F bond ($J_{P-F} \approx 970$ Hz).[53] The singlet at 16.8 ppm is assigned to the product, diisopropyl phosphate (DIP). Degradation of DFP (Scheme 3) is mediated by PHA through the nucleophilic attack of the >N−O−H oxygen in hydroxamic acid on the pentavalent phosphorus of DFP, resulting in P−F bond cleavage and fluorine ion release.

The ratio of the relative signal integrations is proportional to the ratio of the relative concentrations of the corresponding compounds, which allows us to estimate the kinetic parameters of DFP degradation in our experiments. The time-dependent relative degree of conversion, F_t, was defined as

$$F_t = \sum I_r / \left(\sum I_r + \sum I_p \right)$$

(48) Tiller, J. C.; Liao, C.-J.; Lewis, K.; Klibanov, M. *Proc. Natl. Acad. Sci. U.S.A.* **2001**, *98*, 5981.
(49) Aubort, J. D.; Hudson, R. F. *J. Chem. Soc. D: Chem. Commun.* **1970**, *15*, 938.
(50) Bunton, C. A.; Ihara, Y. *J. Org. Chem.* **1977**, *42*, 2865.
(51) Hackley, B. E.; Plainger, R.; Stolberg, M. A.; Wagner-Jauregg, T. *J. Am. Chem. Soc.* **1955**, *77*, 3651.
(52) Endres, G. F.; Epstein, J. *J. Org. Chem.* **1959**, *24*, 1497.
(53) Wagner, G. W.; Bartram, P. W. *J. Mol. Catal. A: Chem.* **1999**, *144*, 419.

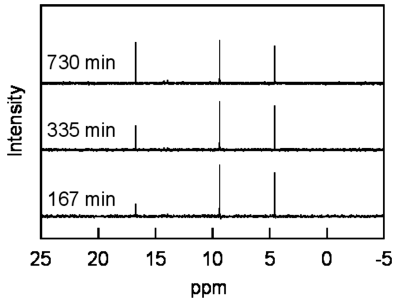

Figure 1. Typical 202.46 MHz ^{31}P NMR spectra showing DFP degradation with time in aqueous solution. $[DFP]_o$ = 5 mM; $[HA]_o$ = 10 mM; 50 mM TES buffer, pH = 7.0; T = 25 °C.

Scheme 3. DFP Degradation Mediated by PHA in Aqueous Solution

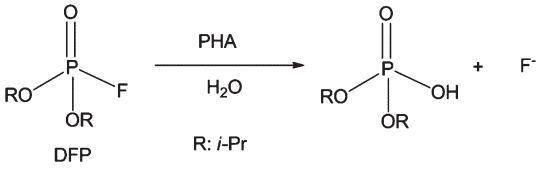

where $\sum I_r$ and $\sum I_p$ are the sums of the integrations of the signals corresponding to the reactant, DFP, and the product, DIP, respectively.

Figure 2 shows the plot of $\ln(F_t)$ vs time for a series of experiments in which the hydroxamic acid concentration, $[HA]_o$, was varied while keeping DFP concentration constant; $[DFP]_o$ = 5 mM. All the experiments were observed to be pseudo-first-order with respect to DFP, as evidenced by the linear fit of the curve $\ln(F_t)$ vs time ($R^2 > 0.99$). The slope yields the observed reaction rate constant, k_{obs}, as described by the equation:

$$\ln(F_t) = -k_{obs}t$$

The observed rate constant without PHA (k_{sp}) was measured to be 1.9×10^{-6} 1/s at pH 7.0, in accordance with previously reported values for the spontaneous hydrolysis of DFP.[44,51] The observed reaction rate increases as $[HA]_o$ increases. In the case of the PHA-aided hydrolysis, the observed reaction rate consists of the PHA-aided and spontaneous reaction rate contributions:

$$r_{obs} = r_{PHA} + r_{sp} \text{ or } \frac{d[DFP]}{dt} = -k_{obs}[DFP]$$

$$= -k_{PHA}[DFP] - k_{sp}[DFP]$$

$$k_{PHA} = k_2[HA]_o$$

Figure 3 shows the curve of k_{PHA} vs hydroxamic acid concentration, $[HA]_o$, in which k_{PHA} is obtained by subtracting the spontaneous term, k_{sp}, from the observed overall reaction rate, k_{obs}. The slope of the linear fit of this curve ($R^2 > 0.99$) yields the second-order rate constant, k_2, which was determined to be 5.1×10^{-4} 1/(M s) for DFP hydrolysis mediated by PHA at pH 7.0. Given that the reaction rate is significantly affected by solution pH,

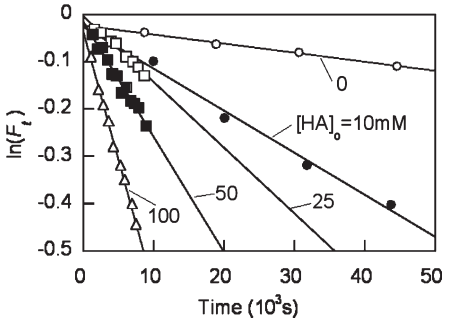

Figure 2. Kinetics of DFP hydrolysis in the presence of PHA in aqueous solution. $[DFP]_o$ = 5 mM; 50 mM TES buffer, pH 7.0.

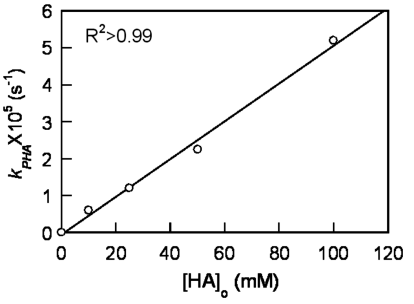

Figure 3. Effect of initial hydroxamic acid concenration $[HA]_o$ on the observed reaction constant for DFP hydrolysis in aqueous solution. $[DFP]_o$ = 5 mM; 50 mM TES buffer, pH 7.0; spontaneous hydrolysis of DFP $k_{sp} = 1.9 \times 10^{-6}$ 1/s at pH 7.0.

the nature of the reaction medium, temperature and pK_a of hydroxamic acid compounds,[49,50,54,55] it is difficult to compare directly the reactivity of PHA with that of small molecular weight hydroxamic acid compounds. On the basis of the reported data, we estimated that the second order rate constant for the DFP degradation via hydrolysis by isonicotinhydroxamic acid methiodide (pK_a 7.8) in aqueous solution at pH 7.0 is on the order of 10^{-3} 1/(M s).[51] Therefore, the reactivity of PHA (pK_a 7.5) toward DFP degradation in this study is comparable to that of isonicotinhydroxamic acid methiodide, a small molecular weight hydroxamic acid compound.

It is well-known that amines and their derivatives can decompose OPs via a general base catalyzed hydrolysis.[56,57] Since antimicrobial poly(*N*-vinyl guanidine) (PVG) is a strong polybase bearing amine groups, it can degrade DFP catalytically as well.[44] To compare the reactivity of PVG with that of PHA, the reaction kinetics of PVG with DFP under identical conditions with the same concentration of functional groups (e.g., $[VG]_o = [HA]_o$) was conducted. The k_{PHA} and k_{PVG} values obtained after subtracting the spontaneous hydrolysis term were 5.5×10^{-5} 1/s and 7.7×10^{-6} 1/s, respectively, at pH 7.0 with $[DFP]_o$ = 5 mM and $[VG]_o = [HA]_o$ = 100 mM. These values indicate that the reactivity of PHA toward DFP is 7-fold higher than that of

(54) Stolberg, M. A.; Mosher, W. A. *J. Am. Chem. Soc.* **1957**, *79*, 2618.
(55) Ghosh, K. K.; Satnami, M. L.; Sinha, D.; Vaidya, J. *J. Mol. Liq.* **2005**, *116*, 55.
(56) Wagner-Jauregg, T.; O'Neill, J. J.; Summerson, W. J. *J. Am. Chem. Soc.* **1951**, *73*, 5202.
(57) Epstein, J.; Cannon, P. L.; Sowa, J. R. *J. Am. Chem. Soc.* **1970**, *92*, 7390.

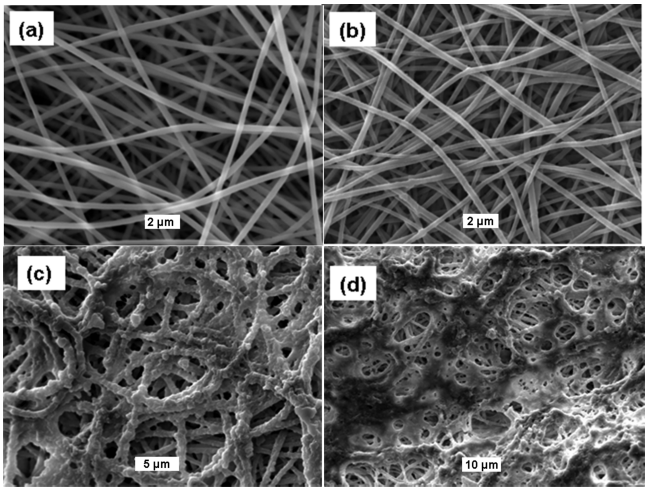

Figure 4. Typical SEM images of (a) prefabricated PAN fiber mat (scale bar: 2 μm). (b) Functionalized PAN fiber mat $(PVG/PHA)_{10}$ (scale bar: 2 μm). (c) Functionalized PAN fiber mat $(PVG/PHA)_{20}$ (scale bar: 5 μm). (d) Functionalized PAN fiber mat $(PVG/PHA)_{30}$ (scale bar: 10 μm).

PVG. Therefore, the reactivity of the PHA/PVG LbL coatings is primarily due to the presence of PHA rather than that of PVG.

Multifunctional Protective Fabrics. LbL electrostatic assembly involves alternate adsorption of oppositely charged materials to construct the ultrathin coatings. PHA is a weak polyelectrolyte with pK_a of 7.5,[29] producing a negatively charged species at pH 9.0. Antimicrobial PVG is a strong polycation. The protonated PVG possesses a pK_a of 13.4 and is positively charged over a broad range of pH.[44] Electrospun fiber mats enable the generation of porous fabric scaffolds with tunable, high specific surface area (1−100 m^2/g) and surface properties. A broad range of electrospun polymer fiber mats have been demonstrated to be effective substrates for LbL-assembled, titanium dioxide-based functional coatings for protection against toxic industrial chemicals or mustard agents.[38,39] Herein, we have selected the commercially available polymer, PAN, as a support matrix of electrospun fiber mats. Figure 4a shows a typical SEM image of PAN fiber mats electrospun from 10 wt % solution of DMF. The average diameter of the PAN fibers is about 350 nm with the fiber size ranging from 250 to 500 nm. The measured BET surface area of PAN fiber mats is about 15 m^2/g. The prefabricated PAN fiber mats were treated with low-pressure air plasma for 1 min to introduce negatively charged surface groups prior to LbL coating of functional polyelectrolytes PVG and PHA.[58,59] Figure 4b shows the typical fiber morphology of the functionalized PAN fiber mats with ten bilayers of PVG/PHA, denoted as $(PVG/PHA)_{10}$. Conformal coatings on individual fibers were observed over the fiber mat. The characteristic peak observed at 529 eV (O 1s) in the XPS spectra (not shown) shows the presence of oxygen, which indicates the presence of PHA on the surfaces of functionalized PAN fibers. With twenty bilayers of PVG/PHA coating, denoted as $(PHA/PVG)_{20}$, a rough surface of functional coatings is clearly observed and the functional coatings start to bridge the pore structures in the fiber mats (Figure 4c). As shown in Figure 4d, with 30 bilayers of the functional coating, $(PVG/PHA)_{30}$, approximately 20−30% of pores are filled. One might expect the filling of pores reported above to affect the breathability of the fiber mats. To evaluate this, the water vapor diffusion resistivities of these fiber mats were measured and compared to standard reference material (Figure 5). In Figure 5, the LbL-functionalized fiber mats, $(PVG/PHA)_{20}$ and $(PVG/PHA)_{30}$, exhibit water vapor diffusion resistivity comparable to that of the untreated PAN fiber mats, indicating that the LbL coatings on the fibers do not affect the breathability of the fiber mats even when the surface pores are partially filled; this accords with similar observations by Krogman et al.[39] It also shows that the water vapor diffusion resistivities of the electrospun fiber mats are lower (more breathable) than that of ePTFE membranes. The ePTFE membrane is a standard porous breathable material. Membranes that exhibit water vapor diffusion properties comparable to the ePTFE membrane are excellent candidates for utilization in breathable protective clothing. The measured airflow resistivity of the functionalized fiber mats is 1.4×10^{13} and 1.0×10^{13} $1/m^2$ for $(PVG/PHA)_{20}$ and $(PVG/PHA)_{30}$, respectively. This is 4−5-fold higher than that of untreated PAN fiber mats (2.7×10^{12} $1/m^2$), but 1 order of magnitude lower than that of ePTFE membrane (1.6×10^{14} $1/m^2$). This suggests that the functional coatings occupy the pores of electrospun fiber mats to some extent, which enhances the barrier performance toward convective airflow as compared to the untreated PAN fiber mats, but such pore filling does not significantly compromise water vapor permeability. Thus, all results indicate that LbL-functionalized electrospun fiber mats are highly breathable and suitable for use in protective clothing materials.

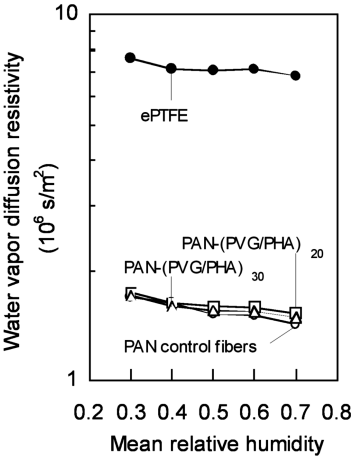

Figure 5. Water vapor diffusion resistivities of (i) control and functionalized fiber mats and (ii) an expanded polytetrafluoroethylene (ePTFE) membrane with pores in the range of 200 nm, a standard reference material for breathable protective clothing. $T = 30$ °C.

The performance of functionalized fiber mats serving as chemical detoxification fabrics was tested with DFP. A DFP mist (3 μL of DFP with 7 μL of air in a 10 μL syringe) was sprayed onto the prepared fiber mat (the mass of dry

(58) Gerenser, L. J. *J. Adhes. Sci. Technol.* **1993**, *7*, 1019.
(59) Dupont-Gillain, C. C.; Adriaensen, Y.; Derclaye, S.; Rouxhet, P. G. *Langmuir* **2000**, *16*, 8194.

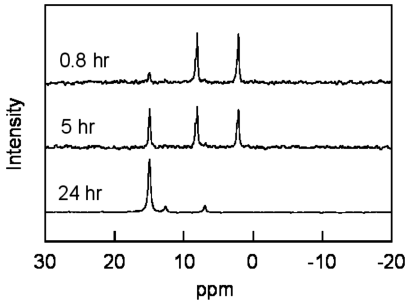

Figure 6. Representative 161.98 MHz ^{31}P HRMAS NMR spectra of DFP mist (3 μL) deposited onto functionalized fiber mat $(PVG/PHA)_{20}$ as a function of time. The mass of dry fiber mat, W_{fo} = 30 mg; water content in the fiber mat, C_w = 1.3 wt/wt; W_{DFP} = 3 mg.

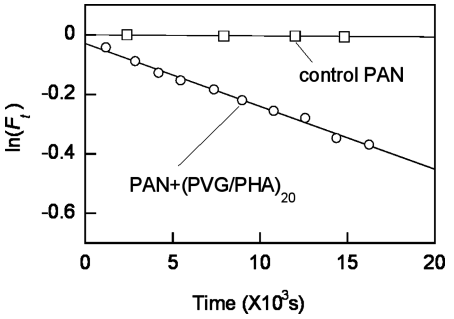

Figure 7. Kinetics of DFP degradation in the presence of functionalized and control fiber mats at 21 °C. The mass of dry fiber mat, W_{fo} = 30 mg; water content in the fiber mat, C_w = 1.3 wt/wt; W_{DFP} = 3 mg.

fiber mat, W_{fo} = 30 mg) to mimic an attack of G-type nerve agents. The DFP degradation mediated by PVG/PHA-functionalized fiber mats was monitored by HRMAS ^{31}P NMR. Figure 6 shows three representative NMR spectra of a DFP-misted fiber mat functionalized with $(PVG/PHA)_{20}$, showing decomposition as a function of time. Doublets at 3.7 and 9.7 ppm ($J_{P-F} \approx 970$ Hz) are assigned to DFP.[53] With time, the doublet peaks for DFP decreased and the singlet peak at 16.6 ppm, assigned to the product DIP, increased. The signals for the reactant and product correspond well with the NMR assessment we have reported previously.[32] The doublets at 12.5 and 6.9 ppm observed after 24 h are attributed to the unreacted DFP that is adsorbed onto the charged polyelectrolyte coating on the fiber surfaces, which shifts the signal positions.[56] Figure 7 shows the DFP degradation kinetics on a PVG/PHA-functionalized fiber mat $(PVG/PHA)_{20}$ as well as an untreated PAN control fiber mat, under identical test conditions (W_{fo} = 30 mg, W_{DFP} = 3 mg, C_w = 1.3 wt/wt, 21 °C). DFP degradation mediated by the PVG/PHA-functionalized fiber mat in the presence of water was observed to be pseudo-first-order with respect to DFP. The observed reaction rate is 2.1×10^{-5} 1/s, which is approximately 60-fold faster than the observed spontaneous decomposition rate of DFP in the presence of the control fiber mat with the same water content. The reactivity of the functionalized fiber mats modified via the LbL electrostatic assembly method is also comparable to that for oxime-functionalized fiber mats prepared via surface oximation reported previously.[32] The advantage of the LbL assembly method is its universality as a means for coating a broader selection of existing polymeric fiber substrate materials compared to the methodology of direct chemical modification of the fiber material, where the choice of material is limited to fiber-forming polymers possessing certain functional groups that can be converted to the reactive groups. The PVG/PHA-functionalized fabrics also demonstrate better reactivity toward DFP compared to XE-555, a commonly used decontaminating, cleaning solution recommended for personal equipment.[53]

The performance of the PVG/PHA-functionalized fiber mats in protecting against bacterial contaminants was tested with a representative gram-negative strain of *E. coli* and a gram-positive strain of *S. epidermidis*.

Table 1. Antibacterial Activity of PVG/PHA-Functionalized Fiber Mats

	bactericidal efficiency (%)	
number of bilayers	*E. coli*	*S. epidermidis*
1	20.0	25.0
5	99.5	99.8
10	>99.9	>99.9
20	>99.9	>99.9

The functionalized fabrics were challenged with airborne bacteria in the form of sprayed mists, to mimic combat situations, as described in the Experimental section. Table 1 shows the bactericidal efficiency of the functionalized fiber mats with different levels of PVG/PHA coating. The bactericidal action of PVG with its large positive charge density, has been attributed to its excellent ability to bind onto negatively charged cell surfaces or cytoplasmic membranes and irreversibly disrupt cell membranes, thereby killing the microorganisms.[60−63] With one bilayer coating, the fiber mat demonstrates only 20% and 25% killing efficiency, respectively, against *E. coli* and *S. epidermidis*. This low activity is attributed to the low concentration of PVG on the fiber surface. It is well-documented that there exists a minimum inhibitory concentration for PVG in aqueous solution (34 μg/mL for *E. coli* and 68 μg/mL for *S. epidermidis*[44]). As the number of bilayers increases, the killing efficiency increases significantly. In the case of five bilayer coatings, the functionalized fiber mats are capable of killing 99.8% of the viable bacteria. With functional coatings of ten or more bilayers on the fiber mats, no bacterial colonies were observed on the mats after the test. We also examined the effect of the last applied coating layer on the bactericidal property of PVG/PHA-functionalized fiber mats. The same bactericidal efficiencies (>99.9%) were observed for functionalized fiber mats $(PVG/PHA)_{20}$ or $(PVG/PHA)_{20.5}$ and $(PVG/PHA)_{10}$ or $(PVG/PHA)_{10.5}$ with either PHA or PVG as the last applied coating layer in electrostatic assembly. This can be attributed to interpenetration between neighboring layers of polyelectrolytes, resulting

(60) Browton, P.; Woodcock, P. M.; Heatley, F.; Gilbert, P. *J. Appl. Bacteriol.* **1984**, *57*, 115.
(61) Gilbert, P.; Pemberton, D.; Wilkinson, D. E. *J. Appl. Bacteriol.* **1990**, *69*, 585.
(62) Pemberton, D.; Wilkinson, D. E. *J. Appl. Bacteriol.* **1990**, *69*, 593.
(63) Khunkitti, W.; Hann, A. C.; Lloyd, D.; Furr, J. R.; Russell, A. D. *J. Appl. Microbiol.* **1998**, *84*, 53.

always in the presence of PVG functional groups in the outer layer of the functional coatings on fiber surfaces.[64−66] A disk diffusion (Kirby Bauer) test was conducted on the functionalized fiber mat $(PVG/PHA)_{20}$ to test for possible release of PVG from the functional coatings to the surrounding environments. No zone of inhibition was observed for the fiber mat after the test, indicating that functional PVG/PHA coatings on fiber surfaces do not release PVG out to the proximity under test conditions, and only kill bacteria on contact.

4. Conclusions

The layer-by-layer electrostatic assembly technique has been applied to electrospun nanofibers and used to fabricate novel, highly breathable electrospun fiber-based chemical, and biological detoxifying protective fabrics and filters based on the reactive polyanion, polyhydroxamic acid, and antimicrobial polycation, poly(*N*-vinyl guanidine). The combination of layer-by-layer electrostatic assembly and the electrospinning technique allows us to take advantage of high specific surface area, light weight, and high porosity of electrospun fiber mats while simultaneously providing the versatility to incorporate different functional polyelectrolytes to achieve multifunctional coatings for simultaneous chemical and biological protection. DFP degradation mediated by a PVG/PHA-functionalized fiber mat was found to be 60-fold faster than observed with a control fiber mat under identical conditions. Furthermore, PVG/PHA-functionalized fiber mats demonstrated potent bactericidal capability over representative strains of *E. coli* and *S. epidermidis* when used as biological protective fabrics. The simplicity of preparation and meaningful performance of the functionalized fiber mats in decomposing nerve agents and bacterial contaminants suggest that they could serve as the basis for a new generation of breathable chemical and biological protective fabrics, filters, and masks. In addition, the LbL electrostatic coating of porous nonwoven materials provides the versatility to generate multifunctional polymer-based membrane materials for other applications.

Acknowledgment. This work was sponsored in part by the Department of the Army, U.S. Army Research Office, under Grant W911NF-07-1-0139. Any opinions, findings, conclusions and recommendations expressed in this article are those of the authors and do not necessarily reflect the views of the U.S. Army Research Office. Partial support was also provided by the DuPont−MIT Alliance.

(64) Picart, C.; Mutterer, J.; Richert, L.; Luo, Y.; Prestwich, G. D.; Schaaf, P.; Voegel, J. −C.; Lavalle, P. *Proc. Natl. Acad. Sci. U.S.A.* **2002**, *99*, 12531.
(65) Wood, K. C.; Chuang, H. F.; Batten, R. D.; Lynn, D. M.; Hammond, P. T. *Proc. Natl. Acad. Sci. U.S.A.* **2006**, *103*, 10207.
(66) Decher, G.; Lvov, Y.; Schmitt, J. *Thin Solid Films* **1994**, *244*, 772.